Distortion Beat Characterization and the Impact on QAM BER Performance

D. Stoneback, R. Howald and T. Brophy

General Instrument

O. Sniezko

AT&T Broadband & Internet Services

Abstract

This paper discusses measurement and analytical results of distortion beat characterization. This analysis received significant level of urgency recently when field tests showed that the traditional methods of characterizing nonlinear distortions (see NCTA Practices[i]) generated in multichannel HFC networks do not allow for an easy prediction of the behavior of digital signals in the same environment. Especially the introduction of higher, more sensitive modulation schemes (256-QAM) made characterization of the impairments of the HFC channel very valuable.

Beat distortion requirements for analog video are based on subjective video perceptibility correlated to the levels of impairments measured according to a standardized test method. For QAM, BER is a more quantifiable measure. To properly characterize the BER degradation analytically, a statistical description of the intermodulation distortion is necessary. The description required is the probability density function (PDF), an appropriate mathematical description for the evaluation of steady state BER performance. Beyond the PDF, the nonstationarity of the distortion process must be considered to capture possible variations of BER as carrier frequency drift varies the statistics.

Using these techniques, BER performance can be analyzed as a function of the variables that contribute to the distortion's parameters - channel map, analog-to-digital signal power ratios, relative carrier phasing, time, and the nonlinearity performance of the channel. This analysis and supporting measurements can be used to optimally align the forward path when the spectrum consists of a composite of analog and digital signals.

INTRODUCTION

The forward path in HFC networks has been proven able to successfully support digital video signals, transporting the information on RF carriers using 64-QAM modulation. This digital modulation format is also called out for carriage of forward path cable modem signals in DOCSIS compatible modems. The power allotted to the QAM signal is implemented by careful consideration of several issues. Among them are the tolerable degradation of analog performance, the minimum levels for proper performance of the QAM signals, and the necessary S/(N+IMD) for 64-QAM link budget. The payload data in 64-QAM applications is augmented with a powerful forward error correction (FEC), mitigating much of the concern with respect to the last item. However, the 256-QAM modulation scheme, to be implemented for higher bandwidth efficiency of the forward path, is more sensitive to impairments. Moreover, as the field tests indicated, higher layer protocols

(for example, protocols for acquisition time) can affect this sensitivity if not implemented properly.

Field Testing

The field testing was conducted in several systems at AT&T Broadband & Internet Services (B&IS) before introducing digital TV 64-QAM signals to ensure adequate quality of the new service. The test results (see examples in Table 1) showed that in the presence of the normal level of other impairments (noise, reflections), the digital signal was not affected if the digital signal level was 50 dB higher than nonlinear distortion levels measured per NCTA practices. For the ratios between 40 and 46 dB, the subjective performance of the digital signals ranged from very good to tiling. For ratios below 40 dB, the digital pictures were either locked or showed heavy tiling.

Digital TV Margin Testing (450 MHz Cascade)

	Levels			Impairments	Digital Quality	Comments
Test Point	Analog NTSC	Digital TV (50-61)	Beat Level: CTB, CSO	Digital/CTB; /CSO		
	dBmV	dBmV	dBmV	dB		
#1	52	42.5	-36	78.5	Very good	
#2	const	37.7	-25.6, -17.6	63.3; 55.3	Very good	
#2	const	37.7	Both @-8.4	46.1	Tiling	CSO as high as CTB, two interferers resulted in higher total interference power
#2	const	37.7	CSO=-18	52.7	Very good	CSO as high as CTB
#2	const	43.7	CSO=-12.3	56	OK	CSO higher than CTB (affected by digital levels)
#2	const	45.7	-9.4	55.1	OK	CSO higher than CTB (affected by digital levels)
#3	ch 36=38	30	-10.3	40.3	Close to tiling	Misaligned, before realignment
#3	ch 36=38	25	-10.3	35.3	Locked	Misaligned, before realignment
#3		25.5	-19.5	45	Very good	After realignment
#3		25.5	-6	31.5	Locked	After realignment
#3		25.5	-13	38.5	Tiling	After realignment
#3		29	-19.4	48.4	Very good	After realignment
#4		40.5	-13.5	54	Very good	Channel 53 has periodicity (5 dB dip)
#4		40.5	-0.9	41.4	Tiling	Channel 53 has periodicity (5 dB dip)
#4		40.5	-7	47.5	Good	Channel 53 has periodicity (5 dB dip)
#4		40.5	-4	44.5	Good	Channel 53 has periodicity (5 dB dip)
#4		46.5	CSO=-10	56.5	Good	Channel 53 has periodicity (5 dB dip)
#4		49.5	CSO=-6.7	56.2	Good	Channel 53 has periodicity (5 dB dip)
#4		40.5	-20.1; -15.6	56.1	Very good	Channel 53 has periodicity (5 dB dip)
#5	ch 36=40.5	ch 50=31.8; ch 61=24.5	-16.1	47.9	OK	10 dB slope (2/47) and roll-off
#5	ch 36=40.5	ch 50=31.8; ch 61=24.5	-3.5	34.7	Tiling	10 dB slope (2/47) and roll-off
#6	ch 36=34.0	ch 50=25.5; ch 61=16.3	-25.5; -28.1	51	Very good	Flat from 2-47, rolling off for digital
#6	ch 36=34.0	ch 50=25.5; ch 61=16.3	-32; -28.1	57.5	Very good	Flat from 2-47, rolling off for digital
#6	ch 36=34.0	ch 50=28.5; ch 61=19.3	-24.7; -25.3	53.2	Very good	Flat from 2-47, rolling off for digital
#7		ch 50=35; ch 61=31.5	-13	48	Very good	
#7		ch 50=35; ch 61=31.5	-4	39	Tiling on 50 and 61	
#7		ch 50=38; ch 61=34.5	-13	51	Very good	

Table 1: CTB & CSO Impairment Sensitivity of 64-QAM Signal (Field Results)

Lab Tests

The field test could not separate other impairments from the nonlinear distortions. To remedy this shortcoming, the tests were repeated in a controlled environment at AT&T B&IS lab in the test setup presented in Figure 1.

The following tests were performed:

1. Sensitivity threshold (minimum input level);
2. Immunity threshold to:
   - Noise (minimum CNR),
   - Single CW carrier (minimum C/I),
   - CTB and CSO generated by unmodulated (CW) carriers, and
   - CTB and CSO generated by NTSC modulated carriers.

The setup allows for separation of the channel on which the tests are performed from the path in which the impairments are generated. This avoids any influence of the impairment generator on the quality of the reference signal. Moreover, the composition of the interference remains the same since the relative level to the reference QAM carrier is adjusted after generation. The only limitation of the test setup was the fact that the impairments were generated in relatively short cascade but they were generated in a well-behaved region of the amplifiers (far from clipping and saturation points).

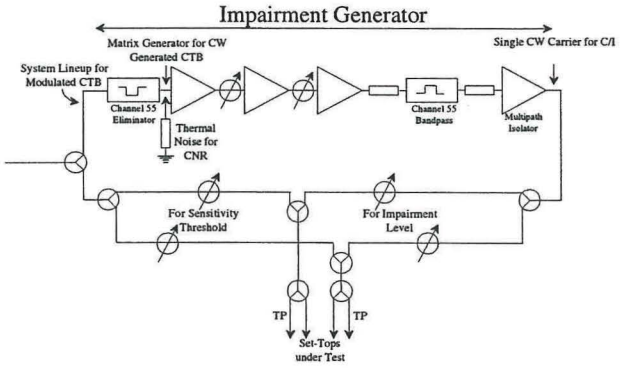

Figure 1: Impairment Test Setup

Impairment Type			Box Type						
			Type 1		Type 2	Type 3		Type 4	
			#1	#2		#1	#2	#1	#2
	Conditions	Units	Impairment Level for Just Perceptible Visibility						
CNR	at -6 dBmV signal to box	dB	22.3	23.0	23.2	22.1	22.8	23.3	24.5
C/I (CW)	at -6 dBmV signal to box	dB	22.8	20.9	23.0	24.0	24.6	22.6	22.1
C/CW CTB	at -6 dBmV signal to box	dB	30.7	NA	36.6	NA	NA	NA	NA
C/Modulated CTB	at -6 dBmV signal to box	dB	34.6	38.8	40.4	35.0	33.8	40.2	40.9
Plant Conditions: CNR=49.9 dB; C/CTB=59.7 dB; C/CSO=65.7 dB (all referenced to an analog carrier 10 dB higher than QAM carrier)									

Table 2: Lab Test Results for 64-QAM Impairment Sensitivity

The tests were repeated for several types of settops. The differences were related to the signal re-acquisition algorithms. The results are presented in Table 2. They clearly depict the problem: sensitivity to single CW interferer is significantly lower than the sensitivity to the CTB and CSO impairments, which are narrowband in nature. Moreover, the sensitivity to CTB distortions generated by modulated carriers is consistently higher than the sensitivity to CTB distortions generated by CW carriers. Both these results show that the NCTA based

method of characterizing nonlinear composite distortion is insufficient for digital signals. Additionally, the tests showed that the sensitivity to the composite nonlinear distortions could be affected negatively by careless selection of the signal acquisition algorithms.

Field Tests with 256-QAM Signals

The field test were repeated jointly by AT&T B&IS and GI in a different plant (high quality) with 256-QAM signals. The test setup is presented in Figure 2. The 256-QAM signal was set at the headend to -6 dBc relative to adjacent analog video carriers. Upper and lower adjacent channels contained analog video. A Wavetek sweep was on the system during the first night of testing but was removed for a repeat test the second night.

The results of this test are presented in Table 3. The only problems were experienced on the node that showed CTB and CSO higher than –60 dBc (node 76) as referenced to the level of analog carrier. This corresponds to 54 dB ratio between the level of digital carrier and the level of impairments (note that both CTB and CSO are high and their effect is cumulative). The repeated test showed the same results. This unexpected outcome (relatively good CTB and CSO) supports the need for additional characterization of the bursty behavior of the composite nonlinear distortions.

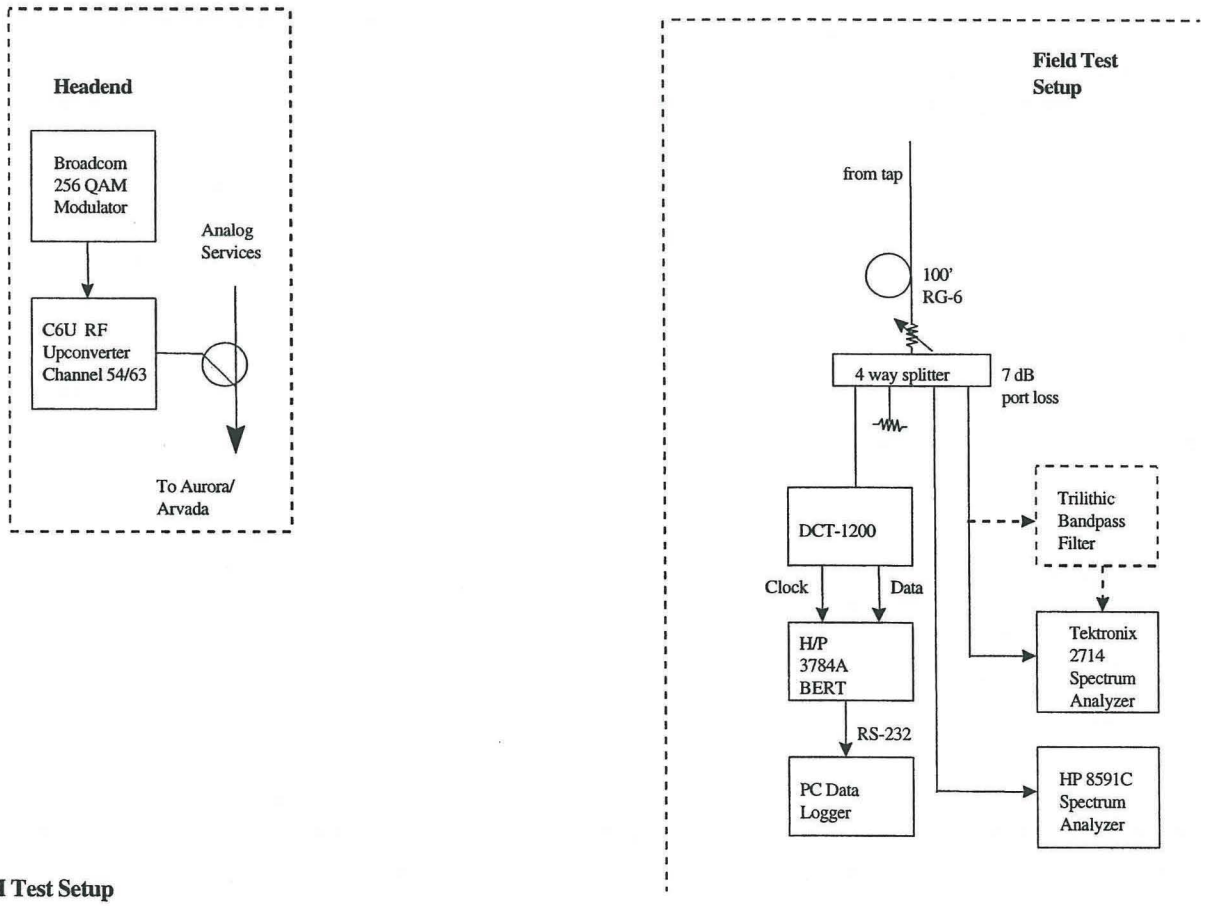

Figure 2: Field Test Setup for 256-QAM Signals

256-QAM test results summary									
	Node 24	Node 32[1]	Node 39	Node 42	Node 43	Node 76	Node 95	Node 99	Node 76
Digital C/N in 6 MHz b/w using channel 63	37.2 dB	>32.0 dB[1]	39.1 dB	35.9 dB	40.3 dB	36.4 dB	36.4 dB	39.6 dB	retest
Digital level into DCT for BERT test, in 5.35 MHz b/w[2]	-3.6 dBmV	-12.9 dBmV	-2.6 dBmV	-1.9 dBmV	-2.5 dBmV	-4.1 dBmV	-7.9 dBmV	-2.6 dBmV	
BERT test duration in sec	1800	1800	1800	1800	1800	43133	1800	1800	55229
Errored seconds	0	0	0	0	1	22	1	0	29
Total bit errors	0	0	0	0	26198	166023	23751	0	230070
% error free seconds	100	100	100	100	99.94	99.95	99.94	100	99.95
Average digital level relative to channel 61	-7.3 dB	-6.5 dB	-7.4 dB	-6.3 dB	-6.5 dB	-7.5 dB	-6.2dB	-7.2 dB	
Channel 3 carrier level[2]	1.8 dBmV	-4.3 dBmV	5.1 dBmV	3.5 dBmV	9.6 dBmV	7.0 dBmV	1.0 dBmV	5.8 dBmV	
Channel 31 carrier level[2]	3.9 dBmV	-3.2 dBmV	6.8 dBmV	6.4 dBmV	6.5 dBmV	5.2 dBmV	1.2 dBmV	7.6 dBmV	
Channel 61 carrier level[2]	3.7 dBmV	-6.4 dBmV	4.8 dBmV	4.4 dBmV	4.0 dBmV	3.4 dBmV	-1.7 dBmV	4.6 dBmV	
Analog C/N: channel 3, measured in service	45.3 dB	45.1 dB	47.8 dB	45.6 dB	46.2 dB	45.2 dB	46.3 dB	45.2 dBmV	
Analog C/N: channel 31, measured in service	46.9 dB	45.2 dB	45.8 dB	47.4 dB	48.8 dB	47.8 dB	47.0 dB	46.2 dBmV	
Analog C/N: channel 61, measured in service	46.1 dB	44.0 dB	46.8 dB	45.0 dB	46.1 dB	46.1 dB	44.9 dB	45.8 dBmV	
Analog CTB: channel 63	64.1 dB	*[1]	67.9 dB	65.0 dB	63.9 dB	59.8 dB	63.3 dB	66.7 dB	
Analog CSO: channel 63	65.0 dB	*[1]	65.8 dB	61.0 dB	64.3 dB	58.4 dB	63.6 dB	66.0 dB	
number of actives	node + 2	node + 4	node + 2	node + 2	node+ 5	node + 4	node + 1	node + 4	

Table 3: 256-QAM test results summary

[1] Noise and distortion readings are not accurate because of low signal level
[2] All measurements are through 100'of RG-6 drop cable and a four-way splitter

MEASUREMENT SETUP

To measure the time domain characteristics of a distortion beat, we decided to use a spectrum analyzer as a tuned receiver with the video output from the spectrum analyzer feeding an oscilloscope. In order to fully characterize the time domain information of the waveform, a search was conducted for the fastest oscilloscope with an amplitude histogram feature. A new line of Tektronix oscilloscopes, called Digital Phosphor Oscilloscopes (DPO) is perfectly suited for this task. The DPO feature allows the scope engine to process incoming data at the full rate of the digitizer, without waiting to update the display. The DPO can record about 500 Million points in 45 seconds. Additionally, this scope has the unique ability to output the entire statistics array to a data file. This data file contains information about how often every voltage was "hit" during the test.

A block diagram of the basic measurement setup is shown in Figure 3. The test signals are fed into the Unit Under Test (UUT), filtered, amplified, and displayed on a spectrum analyzer -- just as in a conventional CTB or CSO measurement. The video output connector of the spectrum analyzer is connected to the input of the oscilloscope. After measuring the CTB or CSO on the spectrum analyzer via the normal "NCTA" method, the analyzer is then set to zero span, which makes it function as a tuned receiver, with the output being at the video connector on the back panel. This detected "video" signal is then measured by the oscilloscope.

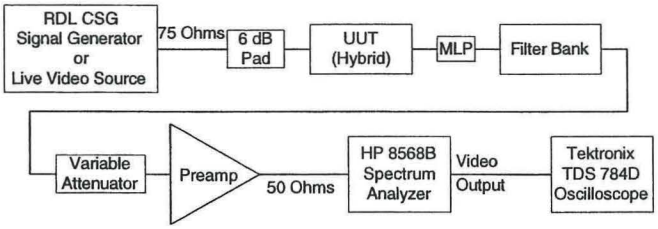

Figure 3: Basic Measurement Setup

Sample oscilloscope displays are shown in Figures 4 and 5. Figure 4 is triggered on a 10 MHz sinewave, which can be seen across the middle of the display. Notice that the tops and bottoms of the sinewave are fuzzy. The DPO records all voltages during the measurement period, so any noise on the waveform will be recorded. In this case 414.97 Million points were measured in about 15 seconds. The left side of the display contains the amplitude histogram. The histogram indicates that the majority of the energy is at the maximum and minimum voltages, which is as expected for a sinewave. Figure 5 shows the same sinewave, but with a free running trigger. To accomplish this, the trigger is set to an unused channel (channel 4) and is set to a high voltage (1.2 V) so that noise will not cause a trigger. Triggering is then set to Auto. Whenever a non-periodic waveform is being measured, it is desirable to not trigger on a particular voltage, since such triggering would cause the histogram data to favor voltages that occur near the trigger voltage. All the CTB and CSO beat measurements were done with a free running trigger. Figure 5 shows that the histogram does not change, but no exact waveform is visible. The color (or shade of gray) of the waveform indicates how often a particular point on the display is hit, with blue being very seldom and red being often.

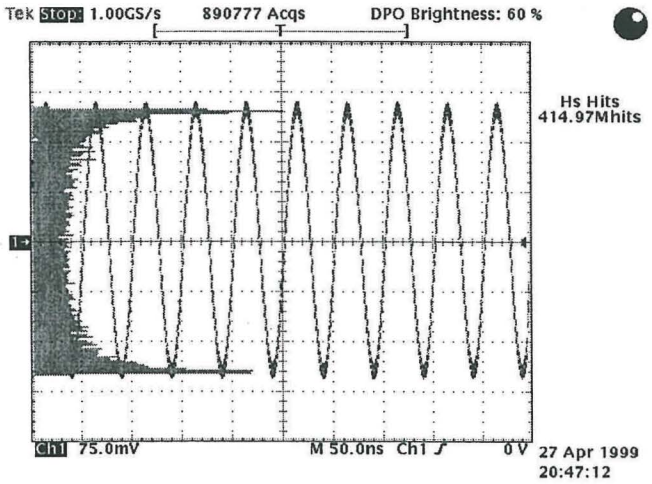

Figure 4: Oscilloscope - Triggered

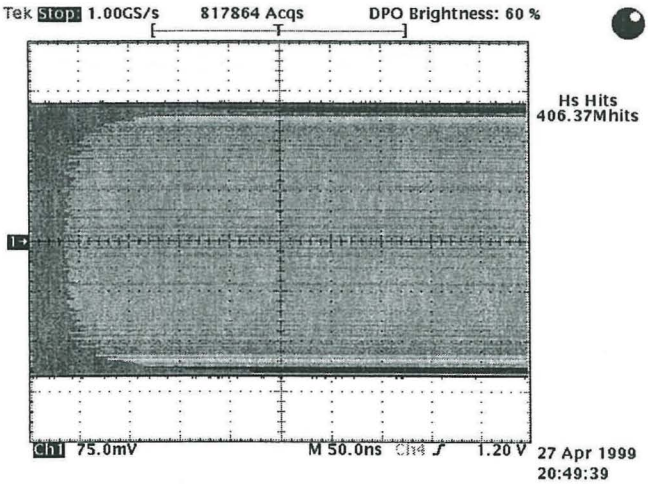

Figure 5: Oscilloscope - Not Triggered

The jaggedness of the histogram displays seem to be caused by inaccuracies of the scope's A/D converter. We did several measurements of various waveforms, including several amplitudes

of noise and discovered that the peaks and valleys of the histogram display are always at the same pixels, regardless of the input signal or the volts/division setting of the channel. We concluded that least significant bit (LSB) accuracy of the A/D was to blame for this phenomena. Although LSB inaccuracy has a minor effect on the amplitude of a signal, having wider and narrower pixels (due to LSB inaccuracies) will be immediately evident on an amplitude histogram.

A second measurement recorded in addition to a histogram is a long time domain record of a distortion event. We choose to save a 130,000 point waveform. For each type of distortion being characterized, several 130,000 point waveforms were saved at various trigger levels. This data is useful for an FFT analysis of the spectral components of the distortion and will be discussed later.

Special Equipment Features

There are several important equipment features and setup tricks in addition to the already mentioned special features of the Tektronix DPO oscilloscope. Many of these irritating gotchas were not noticed until many weeks of data had been collected. The most serious issues are mentioned below.

Getting a reliable, calibrated waveform out of the "video" port of a spectrum analyzer is not a trivial exercise. Very few analyzers provide an accurate, high bandwidth, analog representation of the displayed waveform. We first tried to use an HP 8591C portable spectrum analyzer's video output port. (The video port we are referring to here is the one with an analog representation of the detected waveform, not the composite video port used to display the signal on an external TV monitor.) Everything seemed to be working fine, until we started changing reference levels and dB/division. We quickly realized that the voltage at the video port was not tracking the amplitude displayed on the CRT. This led to several conversations with the experts at HP, where we learned that the video output port on the 8591 is before scale factors and calibration data are applied. As a result, it is essentially useless for the measurements we wanted to make. Upon further questioning we discovered that the 8568 (and 8566) are some of the few units that actually do all the scaling, log amplification, and calibration corrections in the analog circuitry. As a result, the video output port accurately matches the displayed values over all scale factors and reference levels. All the newer equipment has "cheaper" analog circuitry, which is corrected by digital processing. So, there is a reason to keep that old test equipment around!

Another caveat is that the video output connection on the back of the 8568 spectrum analyzer is not designed to drive a low impedance load. For many weeks we collected what we thought was valid data, but were unable to solve some correlation problems. We then realized that the oscilloscope had been set to terminate the video connection in 50 ohms. Normally, this would be good engineering practice. However, the output impedance of the 8568 is not low enough to support a 50 ohm termination, and as a result, the values displayed on the scope did not match the values displayed on the spectrum analyzer.

The voltage gain settings on the scope are also very important. The video signal from the analyzer can go a couple millivolts below zero volts. Since our goal was to develop accurate probability functions and, ultimately, to take FFT's of time domain waveforms, we did not want to clip the waveforms. Thus, we set the ground reference of the scope to be 0.5 graticules from the bottom, instead of being at the bottom. Since there are 8 vertical graticules on the scope (with 7.5 being used) and 10 on the analyzer, there are 0.75 scope graticules per analyzer graticule. Thus, if the analyzer is

reading 10 dB/div, the data will appear on the scope as 13.33 dB/div.

We had a couple other issues with the analyzer. The first 8568 we used had an abnormality in the video output connection. The output signal favored certain low voltages. We discovered this by measuring noise and noting a spike in the response. We never found the cause -- we just got a different 8568 and started over. Also, the 8568 applies correction factors to the analog circuitry. Thus, more accurate results can be displayed on the screen and exported via the video connection if the user calibration is performed and is turned on.

Measurement procedure

The first step to making measurements is to calibrate the equipment. This includes making sure all factory calibration is within specifications, performing any necessary user calibration routines, and setting the proper gains and levels. All user calibration routines should be run. The HP8568 routine (Recall 8, Recall 9, Shift W) must be specifically turned on to be active. Every time the "instrument preset" is used, the calibration data is turned off. The user must turn it on again.

Next, the scope must be set up. The gain of the scope must be adjusted so that the values displayed on the scope match the values displayed on the analyzer. The vertical offset must be set to -3.5 div, and the vertical gain adjusted such that a signal displayed on the reference level of the analyzer is displayed on the top graticule of the scope. Triggering must be set to an unused channel at a high voltage and be in "auto" mode.

Data can now be collected. The spectrum analyzer should be tuned to the distortion and the level of the distortion measured according to the NCTA Recommended Practices (we generally use Resolution Bandwidth (RBW) = 30 kHz, Video Bandwidth (VBW) = 30 Hz, and Span = 500 kHz). The difference between the distortion level and the noise floor should be noted. Then, the RBW and VBW are set as desired for the histogram measurement and confirmation is made that the noise floor is still sufficiently below the signal being measured. Next, the reference level and dB/div (if in log mode) are adjusted as desired and the histogram is measured on the scope. It will take several attempts to get a reference level that allows signals to fill the scope display without allowing some peaks to go past the top of the display. Never forget to record the reference level of the spectrum analyzer. It will be required for data processing and does not show up in the scope plot.

Processing the data

In DPO mode, the oscilloscope stores a two-dimensional array, which contains the number of times each display pixel was "hit" by the waveform. This histogram file (called an "imh" file) can be converted to a tab delimited file with a conversion program. When the data is imported to a spreadsheet, each voltage is in a column, with the lowest voltage in the left column and the highest voltage in the right column. There are 200 columns which map to the 8 divisions on the screen. Thus, there are 25 pixels (columns) per vertical graticule. Each row represents one pixel across the horizontal axis (time axis) of the oscilloscope screen. There are 500 rows which map to the 10 divisions on the screen . Thus, there are 50 pixels (rows) per horizontal graticule.

To process the data, the sum of each column is calculated. This gives a one-dimensional array containing the number of hits at each voltage. The voltages in the array are the scope's voltages, not the voltage of the waveform being measured. Each scope voltage must be mapped to its equivalent signal voltage

at the spectrum analyzer, by accounting for the fact that there are 7.5 divisions on the scope and 10 divisions on the analyzer. Additionally, if the analyzer is in log mode, the dB values must be converted to voltages. Be careful to calculate using the correct impedance (50 or 75 ohms).

To normalize the data, the number of hits at each voltage is divided by the total number of hits. This yields the probability for each voltage, $P(x_i)$, where x_i = the voltage at each data point. The total probability equals 100% ($\sum_i P(x_i) = 1$). The cumulative distribution can be obtained by summing the probability $P(x_i)$ from the first column to the current column.

The probability density function (PDF) requires several calculations to assure unity area under the curve. When log data is converted to linear data, the linear points will no longer be evenly spaced (x_i will not be constant). Without correction, closely spaced x_i will be under-represented on the PDF curve, while widely spaced x_i will be over-represented. To correct this, each data point, $P(x_i)$, must be divided by the difference between the current voltage and the previous voltage, Δx_i. The PDF is obtained by plotting the result $(\frac{P(x_i)}{\Delta x_i})$ for each x_i. By plotting the PDF per millivolt as described above, linear data with a constant Δx_i and logarithmic data with a variable Δx_i will both appear equal. In addition, unity area is guaranteed since $\sum_i \frac{P(x_i)}{\Delta x_i} * \Delta x_i = \sum_i P(x_i) = 1$.

Finally, it is necessary to scale the measured voltages so that CTB and CSO beats with different average powers can be normalized to each other. A CTB with a power of -62 dBm will have a different PDF than a CTB with a power of -65 dBm. This can be corrected by always hitting the analyzer with the same beat power or by mathematically correcting the data. We chose the latter because making all measurements hit the analyzer at the same level seemed to be problematical. To scale PDF data taken in log mode, we add or subtract the dB correction factor to all the powers. To scale PDF data taken in linear mode, we calculate the multiplication factor associated with the desired correction and multiply all the voltages by that factor.

$$\text{Multiplication Factor} = 10^{\left(\frac{\text{Correction Factor (dB)}}{20}\right)}$$

CTB AND CSO BEAT FINDINGS

One of the first steps to measuring CTB beat characteristics was to choose a proper resolution bandwidth for the spectrum analyzer and sweep time for the scope. Figure 5 shows PDF's of the CTB produced by a hybrid at 547.25 MHz when loaded by 82 channels from 55.25 to 541.25 MHz. Unless otherwise noted, all of our tests used the same 750 MHz push-pull hybrid. After rescaling the amplitude data to account for the slightly higher total average power measured by wider RBWs, all the PDF's fall on top of each other. This is shown in Figure 5.

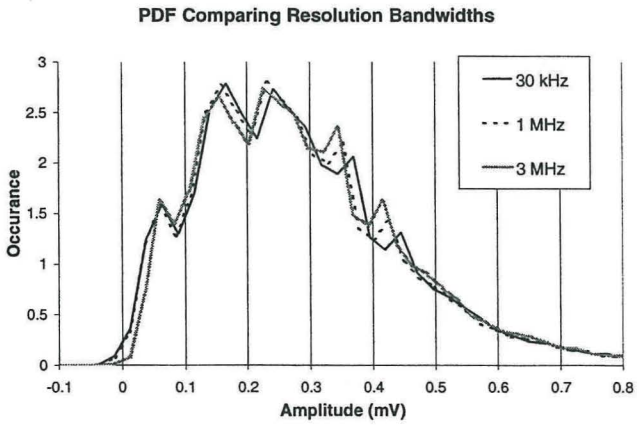

Figure 5: Resolution Bandwidth Comparison

We decided that in order to capture high frequency transient events, it is desirable to use a large RBW. However, larger RBWs allow more noise into the measurement and also capture energy from adjacent beats. As a compromise,

we chose a 1 MHz resolution bandwidth. This bandwidth is wide enough to capture the character of the distortion (including high frequency components), but narrow enough to reject, at least partially, adjacent distortion beats. In addition, we settled on a sweep speed of 5 uSec/div (100 nSec/point) for the scope. This allows frequencies up to 5 MHz to be processed.

A major goal of this paper was to compare the PDF's of CTB and CSO through various devices when stimulated by different loadings of CW or live video signals. This proved to be a huge task. The procedures mentioned previously require very accurate and meticulous measurements. Although the process has been continually refined since its inception over 5 months ago, valid data has only been measured in the last several weeks. In particular, properly scaling the measured voltages so that CTB and CSO beats with different average powers can be normalized to each other is critically important. A 1 dB error here can make one draw the wrong conclusion from a PDF comparison. Most measurements of average beat power are done with the "NCTA" method, using RBW=30 kHz and VBW = 30 Hz. However, the average power of a beat changes when the RBW is increased from 30 kHz to 1 MHz. The amount of this increase is variable depending on the signal being measured, but is generally 1 to 4 dB. PDF's should be scaled according to the power in the 1 MHz measurement, since the data and the scale factor should come from the same conditions. When these findings are compared to the NCTA method, this difference in power will need to be incorporated.

Figure 6 compares two drive levels of live video, one being 3 dB higher than the other All the data is scaled to an average power of -67 dBm (approximately 0.1 mV in 50 ohms). The PDF's clearly show that 0.1 mV is the most likely value. The data at the low drive level was taken several times to assure repeatability. No difference can be found between CTB or CSO at high or low output levels. Figure 7 Compares CW to Live Video. Since our concern is with the high amplitude peaks, which are not readily visible on a linear scale, Figures 8 and 9 show the same PDF's on a log scale. Now the difference between Video and CW loading is evident. Later in this paper, we will discuss how the frequency content of these two signals is also different. We must immediately add that our data collection is continuing and we hope to verify these recent findings during the paper presentation at "Cable 99." A sample of the Oscilloscope display during a histogram measurement is shown in Figure 10.

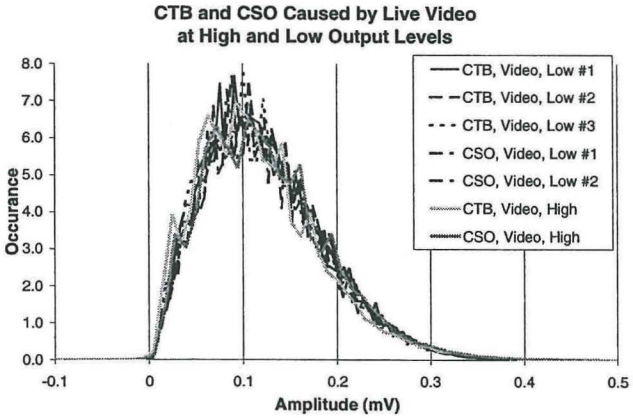

Figure 6: PDF Caused by Live Video

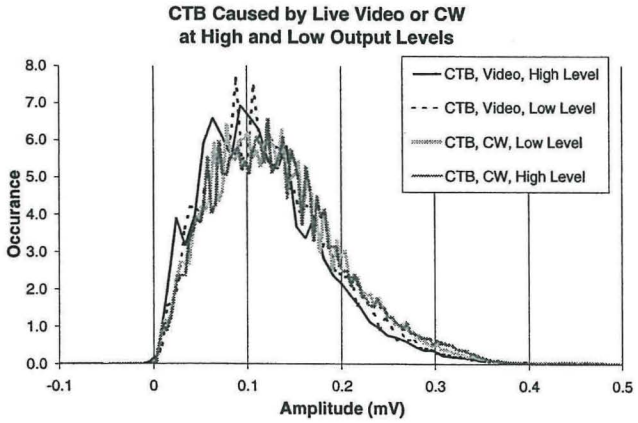

Figure 7: PDF Caused by Live Video or CW

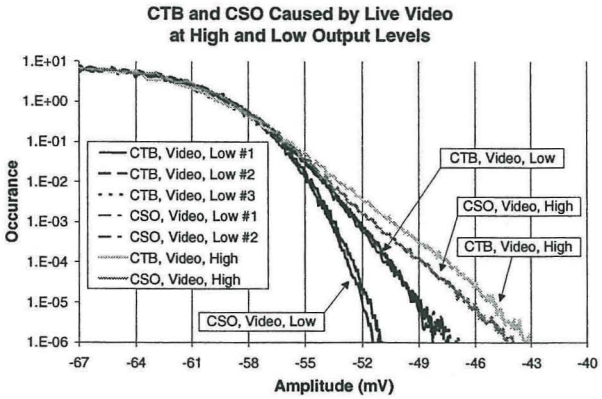

Figure 8: PDF Caused by Live Video (on Logarithmic Scale)

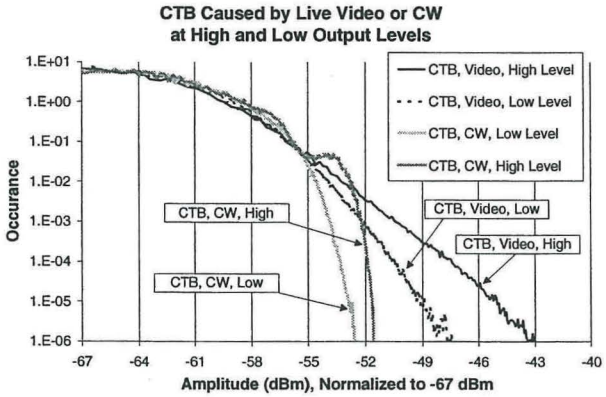

Figure 9: PDF Caused by Live Video or CW (on Logarithmic Scale)

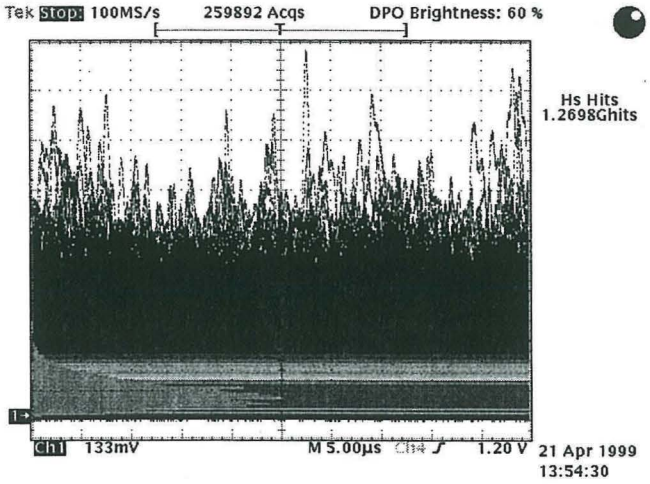

Figure 10: Oscilloscope Histogram Display (CTB of video at high output level.)

BER INTERFERENCE TESTS

In addition to testing the amplitude characteristics of distortion, we did some measurements of the susceptibility of 64QAM and 256-QAM to CTB and CSO interference. The block diagram of the test set-up is shown in Figure 11

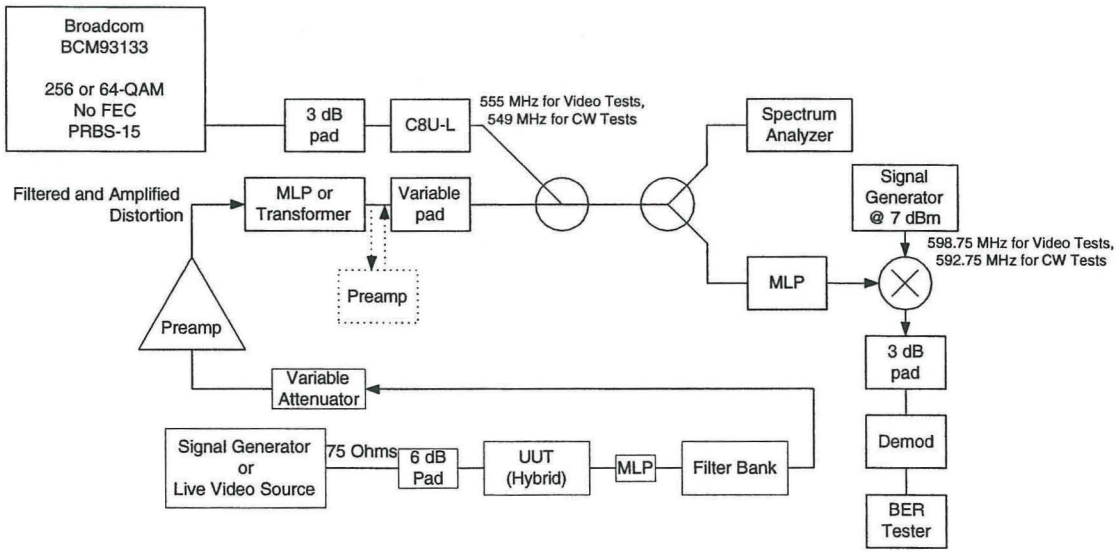

Figure 11: Block Diagram of BER Interference Test

The same UUT (hybrid) was used to create distortion from either a CW or a live video feed. This distortion was filtered, amplified, and combined with the QAM signal at varying levels. At each level, the BER and interference were measured. To get the best possible measurement of the total channel power and the total power of the distortion within the channel, the digital channel power measurement feature of the HP 85721A Measurement Personality in conjunction with an HP 8591C spectrum analyzer was used. This measurement feature provides an accurate measure of the total integrated power between two measurement markers (the 6 MHz channel in this case). The results are presented in Figure 12.

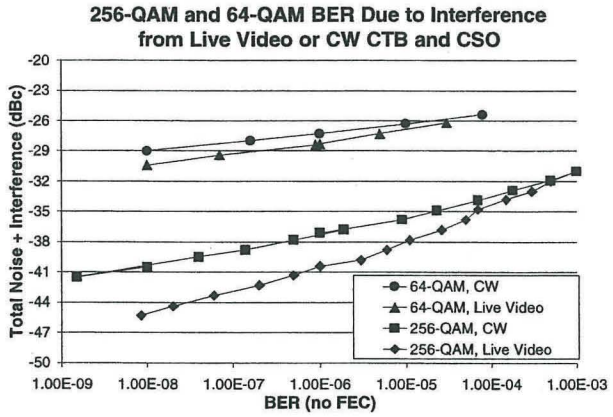

Figure 12: 256-QAM BER

Several important conclusions can be drawn from the results in Figure 12. Most importantly, although 256-QAM is only 6 dB more sensitive to additive white Gaussian noise (AWGN), at BER=10^{-8} it is 14 dB more sensitive to CTB and CSO from live video and 11 dB more sensitive to CTB and CSO from CW. In addition, 256-QAM is increasingly more sensitive to live video (compared to CW) as the interference level drops. Plots of the Live Video or CW distortion compared to the QAM channel at BER=10^{-6} are shown in Figures 13 through 16.

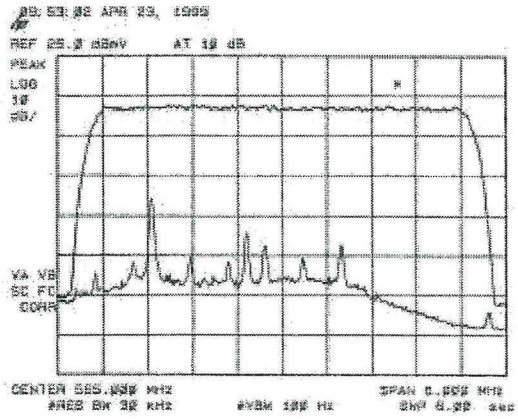

Figure 13: 256-QAM with Live Video CTB and CSO Interference

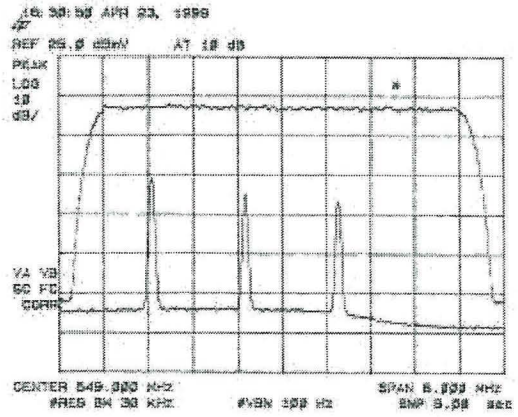

Figure 14: 256-QAM with CW CTB and CSO Interference

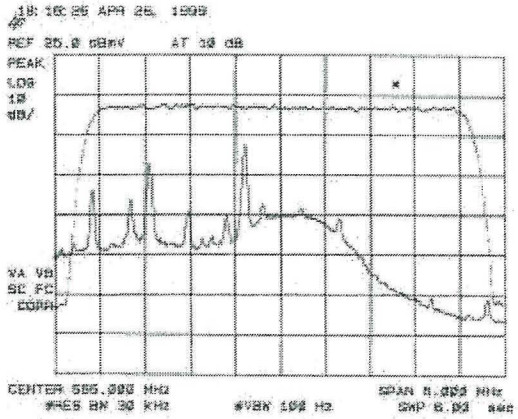

Figure 15: 64-QAM with Live Video CTB and CSO Interference

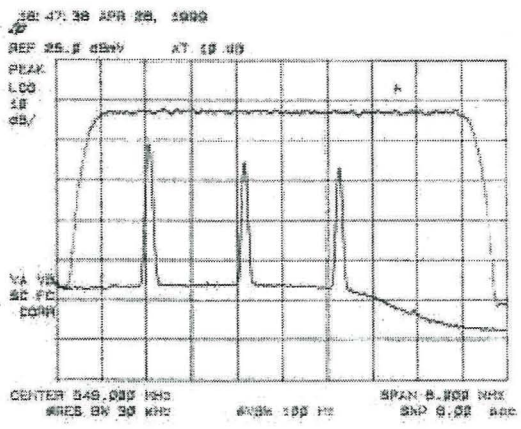

Figure 16: 64-QAM with CW CTB and CSO Interference

PROBABILITY DISTRIBUTIONS

BER

To analyze BER for any degradation type, including simply additive white Gaussian noise (AWGN), a statistical description of the impairment is needed. The "Gaussian" in the AWGN case is that description for common thermal noise. Although seemingly closed form solutions exist for the BER of digital signals in AWGN, these solutions are, in fact, numerical integral solutions. The Gaussian probability density function (PDF) (also called a Normal density), and its cumulative distribution function (CDF) are so commonly used that the expression for writing solutions using the latter has its own function name. By various definitions, it is referred to as the error function. The Gaussian PDF is the best known in the communications industry and many others, and is expressed

$$f(x) = [1/\sqrt{2\pi\sigma^2}] \exp[-(x-\mu)^2/2\sigma^2],$$

where

μ = mean (average)
σ = standard deviation.

The two parameters, μ and σ, completely specify any PDF described as Gaussian, a very important property when used in conjunction with other Gaussian properties in mathematically processing random signals. As such, it is often the case that a Gaussian random variable is abbreviated as $N(\mu,\sigma)$, with "N" standing for Normal. In communications, the noise is AWGN, and typically $\mu = 0$. This is another way of saying that thermal noise has a zero average voltage. The noise power in this case is then σ^2.

For digital communications, the related function often used for evaluating BER is denoted Q(x), where

$$Q(x) = {}_x f^{\infty} [1/\sqrt{2\pi}] \exp(-z^2/2)\, dz.$$

Q(x) is basically the complement of the CDF for Gaussian statistics. For QAM signals, the variable x becomes a function of the SNR, or of the SNR per bit, E_b/N_o. For example, in the 256-QAM case being studied here, Q(x) becomes $Q[(8E_b/85N_o)^{1/2}]$ and the complete theoretical BER expression for performance in AWGN only becomes

$$Pb(256\text{-QAM}) = (15/32)\, Q[(8E_b/85N_o)^{1/2}].$$

Composite Triple Beat

The case of Gaussian noise is well-known and understood, as AWGN is unavoidable in any system, although the source of the noise fluctuations may differ. What separates the BER analysis of different impairments types in digital communications systems is the modulation employed and the statistical nature of the impairment. It is not always easy to characterize an impairment stochastically. Working with PDF's mathematically is straightforward, although at times cumbersome. However, determining what PDF is to be used is not so straightforward. The degradation that occurs may be associated with nonlinear phenomenon, and a function of many variables themselves of which are not easily described mathematically. If there are enough

random variables, none of which are particularly dominant, and they are independent, it is often the case that the Gaussian assumption is valid. This assumption is grounded in the Central Limit Theorem.

For the analysis at hand, the PDF characterization is a two-fold process. First, the distortion beat was captured on a high-speed digital oscilloscope following detection in a spectrum analyzer, and processed as previously described (direct RF detection can also be performed, but would require removal of the deterministic bandpass component of the signal). The scope itself has the capability to perform the histogram function, which has essentially the same information as a PDF, achieved via numerical means. Second, the data captured is exported to a PC and curve fit to determine an appropriate mathematical description. The raw data from the oscilloscope, accessed via software interface, can be loaded into a mathematical analysis program, such as MathCad or Matlab. The data also dumps nicely into Excel, which is also sufficient for much of the processing directly. However, the intricate statistical functions for PDF determination are not as easily implemented, aside from the inconvenience of working with large equations in such a spreadsheet program. Thus, the data captured was then moved into MathCad for further processing.

There are several ways to proceed towards a PDF description. Those familiar with statistics and population sampling may be familiar with a pair of tests known as the Chi-Square test and the Kolmogorov test. The general approach of these mathematical routines is look at a set of data, compare it to an estimated PDF, and determine whether the hypothesized PDF is a good match. There is much more too it than that, as the "confidence" level of the test and "power" of the test are important variables involved in making a determination. These are quantitative parameters. But, the general idea is to utilize known data and compare it to how it should be distributed if it had a certain PDF. The histogram plays an important role in "goodness of fit" testing, as it provides the clues to what PDF's are worthwhile to test. Actually envisioning the PDF fit in a figure is more enlightening. Figure 17 shows an example of captured data (the rough curve), captured and filtered (for smoothness) data, and some overlaid PDF candidates (lognormal, Rayleigh, and F distributions).

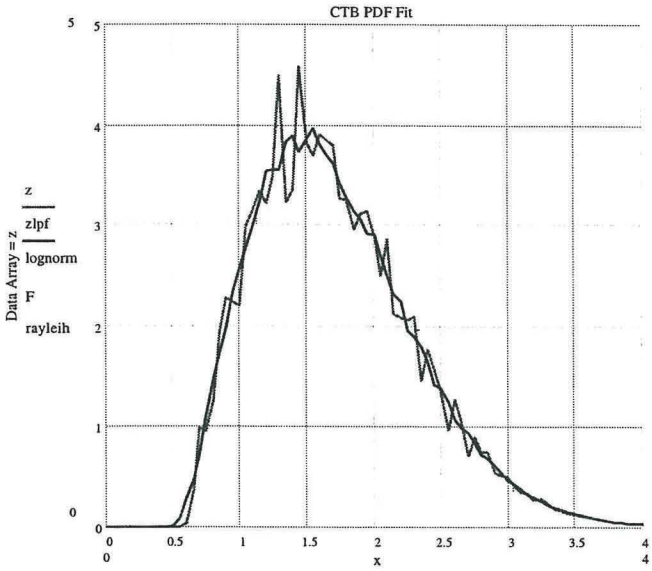

Figure 17: CTB Beat Statistical Fit

As can be seen in the figure, a PDF called the lognormal matches the sampled data well. The lognormal PDF is given by

$$f(x) = [1/\sqrt{2\pi x\sigma^2}]\ \exp[-(\ln(x)-\mu)^2/2\sigma^2].$$

Another PDF with matching characteristics is the Rayleigh distribution, which is given by

$$f(x) = [x/\sigma^2]\ \exp[-x^2/2\sigma^2].$$

In this case, the distribution is also shifted on the x-axis away from the origin. This is likely an artifact of the use of linear detection of the spectrum analyzer for capture. This causes poor

resolution for very small (near zero) amplitudes, but better response at high amplitudes. The higher amplitudes are the ones of most interest for this analysis, as this is what generates errors.

The shapes of these two PDF's vary as a function of their moments (mean and variance are related to the moments of the Gaussian PDF), so it is not unusual that both can be selected to provide a good fit.

It is also valuable to note that, as has been seen previously, the PDF characteristics vary for live video. As was seen, a longer "tail" exists at the higher amplitudes, which is a characteristic more associated with the slower-decaying lognormal function, which rolls off as $[\ln x]^2$ instead of just x^2.

INTERFERENCE MODEL

CW Interference

The impact on BER due to an additive impairment requires determining how detection is impaired when the additional disturbance is included. In the analysis for CTB beat distortion it is easily recognized that the distortion component is an additive effect, inserting an undesired in-band transmission to the 256-QAM channel. There are two other simplifications that will be made to make the analysis tractable:

1. Assume the interference is narrowband
2. Assume the interference is slow

The first item allows us to proceed by beginning with a signal-to-interference (S/I) problem, where the interference is CW, and predicting and measuring BER performance vs. S/I. It is assumed that the CTB beat is sufficiently narrowband enough to behave in terms of bandwidth as a CW signal. Indeed, the 256-QAM symbol rate is about 5.2 Msps, whereas the CTB beat bandwidth is in the tens of kilohertz. The signal BW is thus over 50 times wider than the CTB beat.

The second assumption is not as strong. The amplitude variations of the CTB beats themselves are slow relative to the symbol rate, which is simply repeating that the noisy modulation on the distortion waveform is narrowband. However, consider just a CW interferer. When converted to baseband for symbol detection, the interference represents an additive component with an offset frequency from the center of the channel, creating a sinusoidal component of the noise disturbance. The offset for a CTB beat would be 1.75 MHz, about a third of the symbol rate. This is obviously slower than the symbol rate, but not necessarily to the neglect of the effects of variation during a symbol. However, fortunately, the slow assumption is a conservative one for a noncoherent interferer, since sinusoidal interference would average towards zero by its fluctuations during a symbol period. Coupled with this conservatism is the simplification of the analysis to a tractable problem.

It is worthwhile to repeat again the narrowband property. Because of this assumption, even a noise-like PDF could not be treated in a customary AWGN fashion, in which the analysis is based on an underlying noise density across the bandwidth. In this case, the noise does not have this property.

Geometry of S/I

A CW interferer generates the familiar "doughnut" shape in a constellation. Figure 18 shows this effect for a real 64-QAM signal. The S/I in this case was -23 dBc, and 64-QAM was selected because of the clarity with which the impairment can be seen for 64-QAM, compared to the plot when 256-QAM is used on the same equipment. The doughnut shape represents the phasor rotation of the additive interference

component attached to the end of each vector signal component, which terminates at a constellation point. It is important to note that for this additive impairment, all symbols are effected equally, which simplifies analysis. Some symbols have error boundaries on two sides or three sides, but the effect of the interferer on the location of the constellation point is identical. 256-QAM that can be sensitive, including synchronization functions.

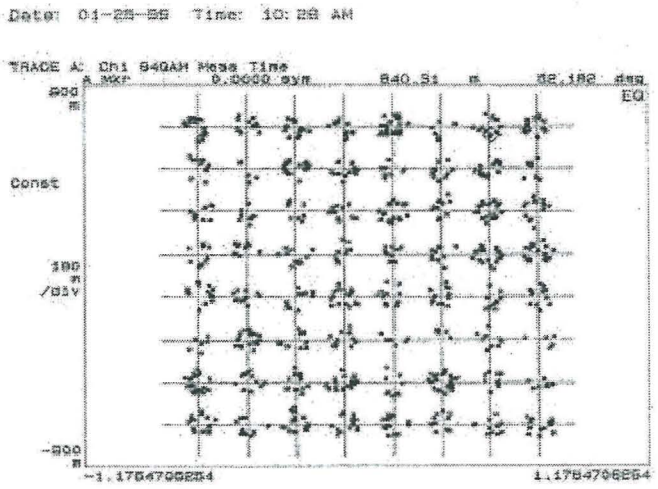

Figure 18: 64-QAM with S/I = 23 dBc and SNR = 40 dB

Modeled performance of 256-QAM is shown in Figure 19 and Figure 20. In Figure 19, virtually noise-free 256-QAM is impaired by a CW interferer of -30 dBc. Despite this very low interference power, the disturbance is visually apparent. This is not surprising when it is recognized that, for 256-QAM, the ratio of boundary distance (the distance between a point on the constellation and the "wall" separating it from an adjacent symbol bin) to the average power is about 22 dB. From this figure, we indeed would expect to see some BER impairment when noise is added to the equation. However, it is important to point out that, without adding noise, this scenario would ideally be error-free. That is, for this CW case, the amplitude of the interferer does not change (nor, equivalently, does the S/I). This error free situation emphasized above considers *only* the detection aspects of the receiver design. In other words, despite the presence of large interference, it assumes otherwise ideal behavior of the receiver right up to the point of making a decision on the symbol. In fact, there are other receiver functions for complex modulation like

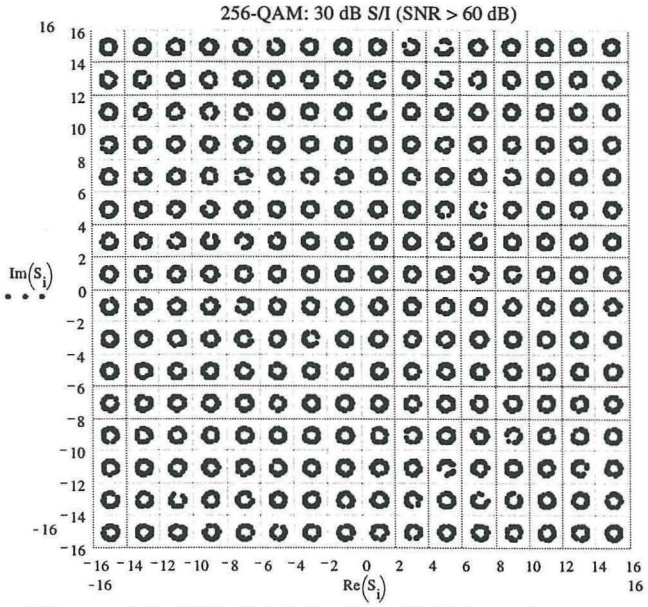

Figure 19: 256-QAM with CW Interference of S/I = -30 dBc and SNR > 60 dB

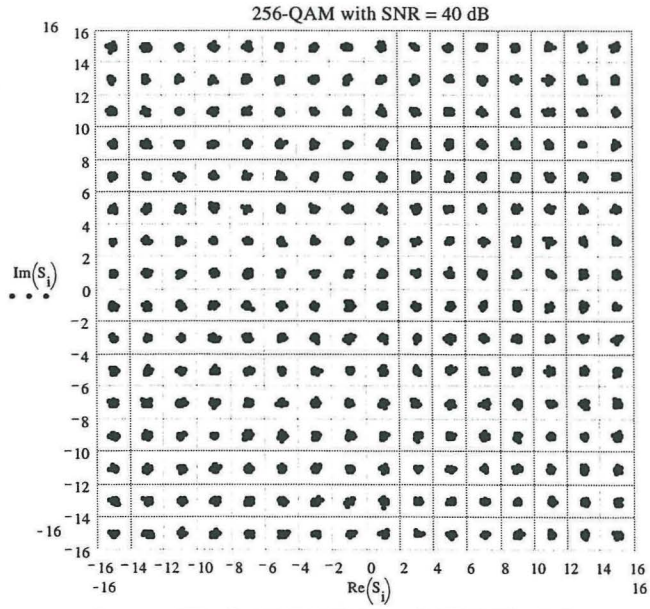

Figure 20: 256-QAM in AWGN with SNR = 40 dB

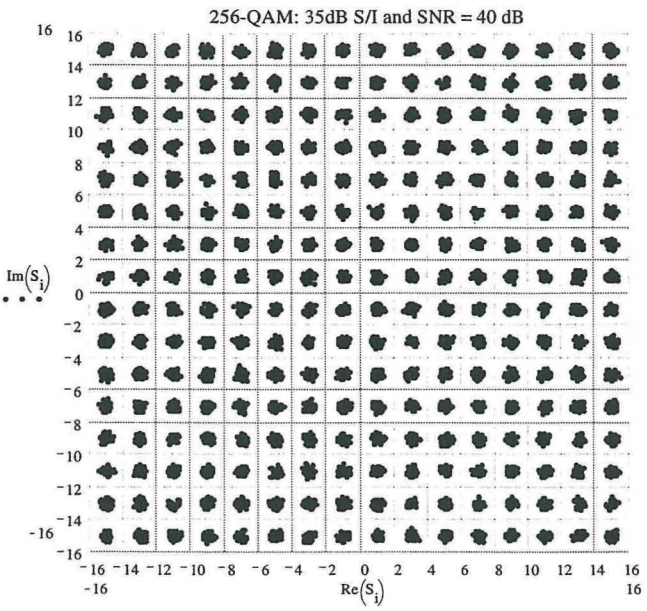

Figure 21: 256-QAM with S/I = 35 dBc and SNR = 40 dB

Figure 20 shows a 256-QAM constellation with AWGN only, with an SNR of 40 dB. In Figure 21, the same SNR is shown, but this time with an additive interferer creating an S/I = 35 dBc. It is apparent that the constellation has been degraded significantly by this amount of interference.

Analytical BER Approach

With a CW interferer, BER analysis can be approached through constellation geometry. Under the slow assumption of the interference effect, the equivalent representation in the constellation is that one point on the "doughnut" represents the impact of the tone on the performance during detection of one symbol. It is further assumed that any point on the circle is equally likely – and thus the phase of the rotating interference phasor is Uniformly distributed.

The result of the interference is that, for a point at some phase ϕ on the circle, the constellation has been shifted towards one decision boundary by [Ki cos ϕ], while the shift has moved it further from the opposite decision boundary by the same amount. Of course, the effect of the moving closer to a boundary dominates the BER effect. This shift can be accounted for by modifying the theoretical BER expression in AWGN by this change in decision boundary distance, which is embedded in the Q(x) argument of the 256-QAM expression.

Since most points in the constellation have four boundaries, we can talk about the above two movements as the in-phase, or I-channel degradation. The quadrature channel, or Q-phase degradation is similar, only based on sin ϕ. Any one of the boundaries being exceeded causes an error, so they are added for composite BER for this symbol. To evaluate the effect of all possible points on the phasor circle means averaging the BER expression over the Uniform phase PDF. That is, BER is calculated for each possible phase and averaging the results over the likelihood of that phase. If it is assumed that all symbols behave the same - not quite the case because of the number of boundaries for the outer symbols in the constellation - then this is all that is necessary to evaluate the symbol error rate. The BER is approximately one-eighth of this, assuming Gray encoded symbols (each adjacent constellation point is different by one bit). Assuming all symbols have four-sided decision boundaries creates a tight upper bound. This is the approach taken, which generated the BER vs. S/I performance plot in Figure 22. We can compare this model to the S/I performance measured on the 256-QAM modem system using CW tones, which is discussed in the laboratory measurement section below.

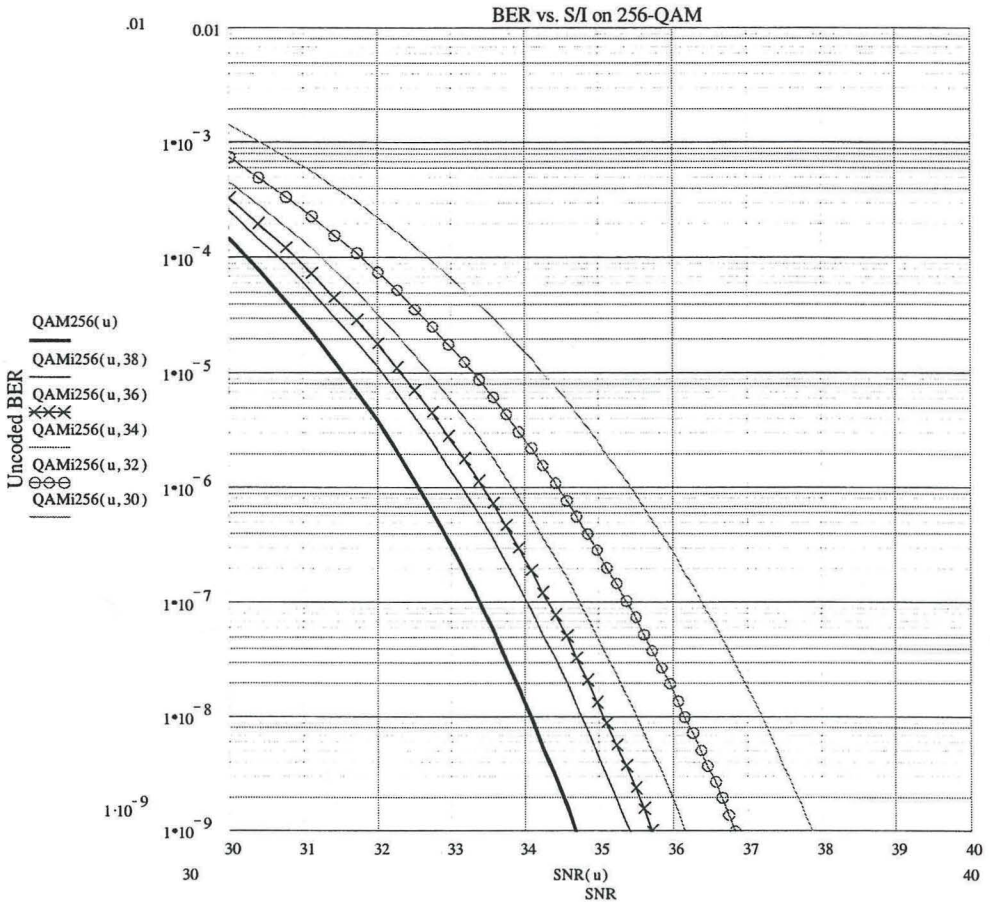

Figure 22: Theoretical 256-QAM vs. S/I

Migrating to CTB

The analysis approach described above is easily adjusted to handle CTB under the narrowband assumption. The adjustment necessary is one that accounts for the amplitude variations of the distortion beat. Since these are, indeed, slow relative to the symbol rate, they can be incorporated to the analysis in the same fashion. Now, however, rather than integrating the modified BER expression with just a change in argument for the interference phase, we include a variable to accommodate another averaging of the expression over a variable amplitude. Thus, the solution becomes a double integral over these two, assumed independent, random variables. The result is an expression in this form:

$$Pb = \int [\int Pe(x,z)\, f(x)dx]\; g(z)\, dz,$$

where f(x) and g(z) represent the phase and amplitude PDF, respectively, of the interference. This latter approach is used to handle the narrowband interferer when CTB is that disturbance.

LAB BER VS. S/I PERFORMANCE FOR CW INTERFERENCE

Measured Performance

Prior to the full-blown RF cascade tests, 256-QAM characterization was performed in terms of signal-to-interference (S/I) testing of 64-QAM and 256-QAM. The point of this

testing was to begin to quantify the effects of distortions falling beneath the digital channels, an essential part of any composite signal optimization program. Table 4 shows a subset of these measurements. Two cases are shown. The first set indicates the effect of a carrier placed right on the center of the channel, where it is most likely also to disturb synchronization of the receiver. This is, therefore, the expected and measured worst case. The second set shows measurements taken at the CTB offset frequency.

64-QAM fo		256-QAM fo		64-QAM fo-1.75Mhz		256-QAM fo-1.75Mhz	
S/I(dbc)	BER	S/I(dbc)	BER	S/I(dbc)	BER	S/I(dbc)	BER
-50	0	-50	0	-50	0	-50	0
-45	0	-45	0	-45	0	-45	0
-40	0	-40	0	-40	0	-40	0
-36	0	-39	0	-35	0	-39	0
-30	0	-38	1.10E-08	-30	0	-38	0
-25	0	-37	1.10E-08	-25	0	-37	0
-24	2.2E-09	-36	9.50E-08	-24	0.00E+00	-36	2.40E-10
-23	8.0E-07	-35	4.70E-07	-23	0.00E+00	-35	2.60E-09
-22	6.7E-06	-34	2.20E-06	-22	3.20E-09	-34	2.20E-08
-21	5.0E-05	-33	7.40E-06	-21	3.50E-07	-33	9.00E-08
-20	4.4E-04	-32	2.20E-05	-20	7.80E-06	-32	4.80E-07
-19	No Sync	-31	6.80E-05	-19	4.30E-05	-31	2.20E-06
		-30	2.00E-04	-18	5.40E-04	-30	9.00E-06
		-29	No Sync	-17	6.50E-03	-29	3.60E-05
						-28	1.30E-04
						-27	4.00E-04
						-26	2.00E-03

Table 4: 64-QAM vs. 256-QAM Signal-to-Interference (CW) Performance

The results of the S/I tests were quite informative, showing 64-QAM, in general, being about 12-14 dB more robust to an interfering CW signal. Note that this is significantly larger than the theoretical 6 dB AWGN difference. This is not necessarily unusual, in that the CW interferer does not represent a Gaussian disturbance. Typical 64-QAM sensitivity to interference shows BER thresholds of error free operation occurring at S/I of between -21 dBc and -24 dBc, depending on location in the band. For 256-QAM, the variation was significantly degraded, to between -34 dBc to -38 dBc. A very small part of this may be modem system implementation loss between 64-QAM and 256-QAM. Measurements were made with the interference placed across the digital band. BER improved as the interference moved away from the center. The results of the cascaded amplifier distortion performance will be compared to these CW interference tests performed at the CTB frequency elsewhere in this discussion.

BER Analysis vs. Measured (CW)

It is of interest to compare the measurements in Table 4 with the results of the BER analytical model developed based on constellation geometry, as described previously. These measurements were done on a clean channel – in other words, the only losses associated with performance are those related to the non-idealities generated by the modem test system itself. There were no distortion beats or optical impairments. The 256-QAM test equipment is as has been described previously. Implementation losses measured in prior characterizations using Modulation Error Rate (MER) concepts (fidelity of the constellation relative to ideal) and estimated detection SNR at the receiver place this number at about 35 dB. Thus, to compare the measured data with the model requires sliding up and down the SNR = 35 dB line on Figure 22.

The figure plots BER performance for ideal 256-QAM, and for S/I = 30, 32, 34, 36, and 38 dB. Obviously, the closest to the ideal curve is the 38 dB case, and so on down to 30 dB. Table 5 shows the comparison in terms of BER value, as well as in the delta in SNR (x-axis difference) between measured and modeled. Note that for zero BER as measured in the first row, the BER value 1E-12 was used to generate an SNR comparison. At error rates this low, very little additional SNR buys another order of magnitude improvement, so it is not particularly significant what very low value is used. For example, just an additional .4 dB of SNR provides a theoretical BER of 1E-13 in AWGN.

The only unusual result seems to be that at worse S/I, the measured data actually is worse than the model, which should be a conservative value. It is suspected that the reason for this is simply that the model overlooks all but the symbol detection aspects, and at lower S/I, other receiver functions are being effected by the interference also. Additionally, care must be taken in accurately assessing the implementation loss of the receiver, such as in controlled tests looking at the vector analyzer MER as done here, or evaluating carefully in a known pure AWGN link.

BER vs. S/I Comparison			
S/I	Analytical BER	Measured BER	SNR Delta
38 dB	4.00E-09	0	1.8 dB*
36 dB	1.00E-08	2.40E-10	1.0 dB
34 dB	4.00E-08	2.20E-08	0.3 dB
32 dB	3.00E-07	4.80E-07	0.2 dB
30 dB	3.00E-06	9.00E-06	0.7 dB

*considering error free as 1E-12
Assumed Imp "Loss" of 35 dB SNR

Table 5: Modeled vs. Measured 256-QAM S/I Performance

Next, a real hardware chain generating actual CTB is considered.

CASCADED RF BER PERFORMANCE TESTS

During the past year, 256-QAM BER measurements have been performed during hardware qualification runs to take advantage of complex chamber setups. This section describes some of these results. All BER results noted are *uncorrected* 256-QAM BER measurements, and we assume a correctable threshold boundary of about 1E-4. This boundary is used as the acceptable BER before error correction that will still provide 1E-8 after error correction. Figure 23 summarizes the results on one particular example cascade. Note that for the RF-only case, SNR is very high, such that BER effects due to AWGN are insignificant for most of the range of digital back-off.

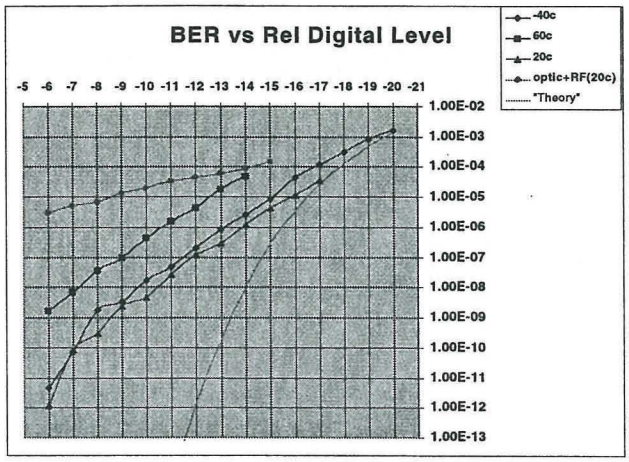

Note: Theory Curve is offset by 3 dB to allow ease of shape comparison, representative of an inherent modem implementation loss. Also, it is based on CNR of a 6 dB fiber link, with CIN treated as an additive Gaussian impairment, and ignoring IMD contributions.

Figure 23: 256-QAM BER, RF and (RF+Optics)

RF Cascade BER Measurements

Low Temperature – Measured digital signal to CTB (S/CTB) = 53 dB for digital @-6 dBc. Distortion performance is best at cold temperatures, and this is reflected in BER. At -40° C, while BER degraded significantly, the QAM level was able to be lowered to the minimum obtainable in the test setup, and the demodulator was still able to lock and hold synchronization. This level was a QAM level relative to analog of about -20 dBc (S/CTB = 39 dB). This is far below what minimum level can be implemented in real plant conditions because of other link degradations, and because of input levels required in the settop box.

The BER degradation curve followed a shallow sloped curve relative to a theoretical plot, which is an unsurprising result considering the overall end-to-end link implementation loss of the system (the dB offset of the curve from ideal). This number, relative to an ideal theoretical curve (as opposed to the one adjusted

here for modem and system implementation losses), is about 7 dB @ 1E-8.

The threshold to which the link maintained a 1E-4 level of uncorrected performance is down to a QAM relative level of -17 dBc (S/CTB = 42 dBc). A 256-QAM level of -6 dBc (S/CTB = 53 dB) resulted in an uncorrected BER of about 4E-12. The complete dynamic range over which 256-QAM can run with FEC applied is then about 12 dB with respect to the RF plant.

Room Temperature – The BER performance at ambient closely follows the cold temperature data, with some slight improvement. There is an increase in thermal noise as temperature increases and there was a slight CTB degradation (.5 dB). Generally, however, the difference in performance between cold and ambient is not significant, varying less than .5 dB on the BER curve to a maximum of perhaps 1 dB.

Over the complete operational range of the link, BER performance was between 1.2E-12 (-6 dBc) and 3.5E-5 (-17 dBc). Thus, the dynamic range of the ambient BER is not degraded compared to cold (correctable dynamic range = 12 dB).

High Temperature – There is an obvious CTB degradation at hot temperature at some frequencies (about 3 dB at the frequency of interest compared to cold), as well as the thermal noise increase.

The additional CTB degradation correspondingly results in less dynamic range of the 256-QAM link. Additionally, the best case BER is now about 1.7E-9 (-6 dBc, S/CTB = 50 dB). The theoretical SNR difference between two extremely low error rates, such as between 1E-9 and 1E-12, is quite small - less than 1.5 dB - so this is not alarming. What it does indicate is that, since CTB is quite low on average in absolute terms, it must have significant peak-to-average effects to cause errors, much like noise, but in a narrowband.

At the minimum QAM level, the BER degrades only to 5E-5, a correctable value, before losing synchronization capability at -14 dBc (S/CTB = 42 dB). This represents a dynamic range window of 9 dB on the RF plant, and still is greater range than within the recommended operational digital "window" of -6 dBc to -10 dBc.

Measured C/I Results and Correlation – As previously mentioned, as part of the effort to completely understand and quantify S/CTB performance in forward 256-QAM links, S/I performance was taken using a narrowband interferer summed with the 256-QAM signal. Measurements show, in the worst case (at center frequency) that when the interferer is in the -38 dBc range, error-free transmission begins to get impaired, and it degrades significantly as S/I moves slowly higher. At what S/I errors begin to occur is within a dB or two across the bandwidth. These results turn out to be consistent with the measured cascade data.

As an example, at hot temperature, measured cascade CTB of about 56 dB occurs. For a digital channel @-6 dBc, this is S/CTB = 50 dB. Although SNR was very high, errors were still counted under all cases of digital level, including this maximum digital level. This is because, unlike CW interference, CTB peak-to-average values are noise-like, measuring in the 12-15 dB range. Of course, the measurement technique used in the cascade runs is average CTB per NCTA. Thus, an S/CTB of 50 dB average would correspond to peak CTB excursions as high as the mid-to-high 30 dB's – precisely where CW tests showed error counts to occur. A peak to average of 15 dB would place the CTB peak at S/CTB of 35 dB. In the hot example above, the measured BER for this -6 dBc setting was 1.7E-9. In the S/I data taken

using a CW interferer placed at the CTB offset frequency, a BER of 2.5E-9 corresponded to the S/I setting of exactly 35 dB.

On the minimum digital level side, which decreased 8 dB in this test, S/CTB degrades to 42 dB average, and 27 dB peak, with a measured BER of 5E-5. The S/I = 27 dB measurement for the CW test was 4E-4. These are about 1.4 dB different on an ideal curve versus SNR.

As one more data point, consider ambient at -10 dBc. Measured BER is about 5E-9. Ambient CTB is 49 dB for digital @ -10 dBc. Peak is then as high as 34 dB. In CW tests where S/I = 34 dB and the tone placed at the CTB beat frequency, measured BER was 2.2E-8. In terms of SNR difference, this is only about .4 dB. The fact that the CW case performs as the slightly worse of the two in each of these examples is explained by the fact that the CTB impairment is an amplitude varying one. Its average level is, obviously, considerably lower, so most of the time the CTB beat spends below its possible peak. But, as expected, it is the peak disturbances that heavily weight the error rate performance. This is the usual situation for transient BER effects, where, for example, the arithmetic mean of 1E-6 and 1E-9 is very much closer to 1E-6.

BER Analysis vs. Measured (CTB)

As in the S/I section for a CW interferer, a BER analytical model was developed. The modification relative to the CW interference case is the use of a random distribution of the amplitude as previously discussed, which was incorporated via a double integral solution over a modified Q(x). This model and measurements made during the RF cascade testing described above is shown in Table 6. The correlation is quite good, and the results indicate the same pattern as the CW case in terms of modem performance. That is, while the modeled performance is based on a conservative bound, the measured performance was actually the worse of the two as the S/CTB decreased. Again, it is expected that this is the result receiver performance in aspects other than detection was also being impacted by the beat disturbance. The modeled performance is based on the same modem system used in the CW case, and thus the same implementation loss.

It is well-known that a Gaussian noise envelope has a Rayleigh PDF, and a convenient property of the beat's noise-like amplitude envelope is the known relationship between the parameters of such noise, and the Rayleigh characteristics. That is, for a known Gaussian PDF, the Rayleigh PDF is completely known also. This is helpful in the analysis, because it is easier to measure the noise statistics, compared to capturing, processing, and scaling the detected envelope. Then, the known envelope amplitude statistics are used to modify the interference "doughnut" radius' relationship to the detection boundary. This relationship is easily calculated as it is a function of the CTB level, the signal power, and the relationship between boundary distance and signal power.

A complete BER vs. S/CTB plot can also be generated as in the CW case. However, convergence problems of the numerical double integral restrict the range of SNR and CTB over which this can be calculated before the calculation must be modified. Thus, this data is observed best available in tabular form at this point. Further numerical methods are continually being considered to enhance calculations efficiency and accuracy for these complex calculations. The case of CTB effects on 256-QAM BER using randomly distributed CW frequencies looks to be a predictable quantity, and important step as the analysis moves into different frequency patterns, optical links, and load variations.

BER vs. S/CTB Comparison			
S/CTB	Analytical BER	Measured BER	SNR Delta
48 dB	6.90E-10	1.20E-12	1.2 dB
46 dB	1.40E-09	3.10E-10	.4 dB
44 dB	3.80E-09	4.80E-09	.6 dB
42 dB	2.60E-08	1.20E-07	.5 dB
40 dB	4.10E-07	1.20E-06	.5 dB
38 dB	6.70E-06	1.20E-05	.4 dB

Assumed Imp "Loss" of 35 dB SNR

Table 6: Modeled vs. Measured 256-QAM S/CTB Performance

One-Hop Optical Link and RF Cascade

For completeness, and to inspire further study, the final 256-QAM BER measurement in the test suite included a single 1310 nm optical link, with a 6 dB link loss, in front of the cascade. The optics added an expected SNR loss of between about .5 dB and 1.5 dB. The other noticeable change was that the BER curve slope became shallower, indicative of another impairment generating its own set of dominant error-generating statistics. The result of this is that the best BER at the -6 dBc value, was only as low as 3E-6. Clearly, another primary impairment - laser clipping - is at work, considering that the ambient RF-only case was 1.2E-12. These points are about 3.5 dB apart on a theoretical curve. The worst case BER that could maintain modem synchronization was a digital signal back-off from analog of -15 dBc, which measured 1.5E-4.

Results for correctable BER *dynamic range* actually do not vary from the ambient case. In fact, the range measured is about a dB wider.

The BER curve behavior can be explained by clipping. While uncorrected BER is impaired significantly, this is, in fact, somewhat encouraging. The characteristics of the clipping events tend to be handled well by sophisticated FEC employed in the forward link. Beat distortion degradation, by contrast, is not as well handled because of the duration of the peak events of the intermodulation, which challenges the capability of the interleaver and Reed-Solomon coding. Again, this is yet another way of pointing out that the CTB envelope is slowly-varying, thus effecting multiple symbols in series.

FFT INFORMATION

Yet another way to crunch the CTB data in a useful way is through the Fast-Fourier Transform (FFT). The FFT tool is valuable for establishing the frequency content in a detected beat. This content immediately points out the "slowly varying" nature relative to the symbol rate, which is also recognizable directly from the spectrum analyzer itself. The FFT tool is also valuable as the frequency distributions are varied. The ability to store, evaluate, and manipulate the frequency content information of the distortion at baseband is useful for several reasons. First, analyzing the characteristics in post processing is easier, flexible, and can be done with varying parameters. Second, regions of interest in the spectrum can individually be focused upon in more detail. For example, any particular region of the spectrum can be integrated to determine the power associated with some portion of the frequency content of the impairment, such as is done with phase noise impairment in carrier tracking loops. Third, it becomes easy to determine the impact on the spectrum through further processing steps, such as in a digital receiver, or through further RF processing steps in a plant. Finally, discrete components extract themselves in an FFT when swept and captured with very low resolution bandwidths not conveniently observed in analog mode.

The FFT of an input analog comb, processed directly by the high speed oscilloscope at RF and through MathCad is shown in Figure

24. A 649 MHz distortion beat is shown in Figure 25. Along with this FFT is a time domain plot of the same from the oscilloscope. On the screen with the time domain trace is the scope's version of an FFT.

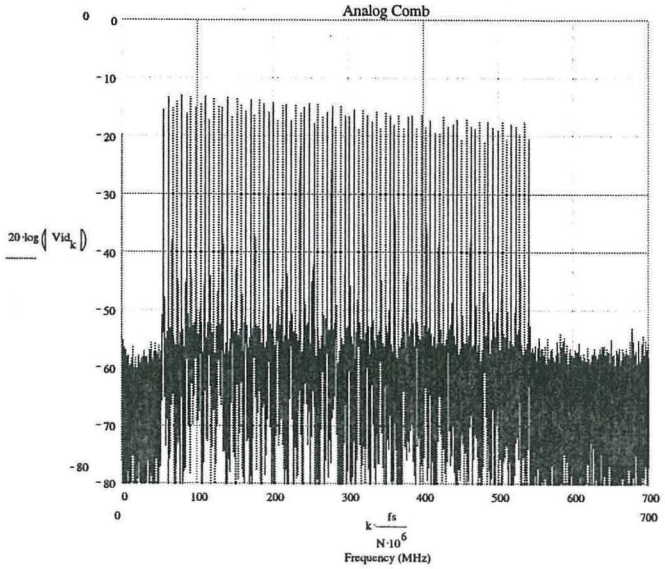

Figure 24: FFT of Forward Analog Comb From Matrix Processed Directly

Of particular note in the processed FFT is the CSO beat at 1.25 MHz. Also, note that the noise floor roll-off occurs at 1 MHz, corresponding to the RBW of the spectrum analyzer detecting the beat. Finally, note that the energy of the CTB is concentrated in the low frequency range, consistent with the fact that the test used a new matrix generator (with non-aged crystals), which thus had frequencies closely aligned (in ppm offset from initial) from one another.

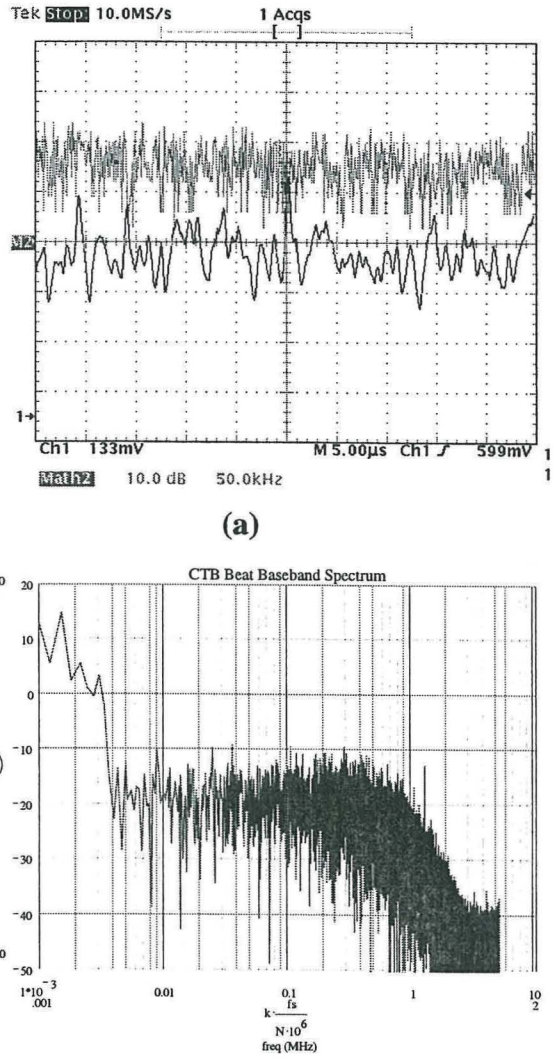

Figure 25: Time Domain Plot (a) and FFT (b) of 649.25 MHz Distortion Beat with CW Carriers

Figure 26 shows a CTB beat at 553.25 MHz when live video is used. Again, the CSO beat and roll-off are apparent. Also appearing in the spectrum is the 15 kHz synchronization information that accompanies real video signals.

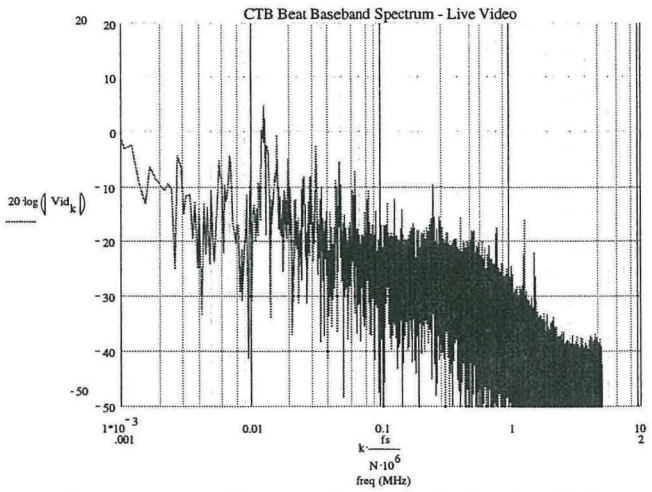

Figure 26: 553.25 MHz CTB Beat FFT using Live Video

As frequency distributions and load levels vary, the effect on the beat amplitude and spectrum - which relates to the duration of beat amplitudes and subsequently the BER - can be evaluated.

CONTINUING EFFORTS

This modeling, analysis, and measurement effort is a work in progress, with many items scheduled for quantification in the months ahead. A subset of the avenues of study are described below.

Frequency Distribution

The majority of data taken for this paper was performed using randomly distributed frequency offsets on the analog channels. Equipment is available to effect the frequency and phase relationship of the channels in any manner desirable. It is known that, as frequencies drift in time, the composite waveform peaks can vary as the drifts align themselves and misalign themselves. This is another way of saying that, statistically speaking, there is a finite, but very small probability that a randomly selected HE will exhibit high peak to average values for some periods of time during its lifetime. The characterization of the distortion when purposely aligning the frequencies and phases is continuing, and the expected higher peak values at more periodic increments has been shown.

These time domain aspects are important in two ways. First, the periodicity implies a deterministic aspect of the peaking that can be used for optimization of the link. Second, they provide information about the dynamics of the symbol error mechanism, which leads to the proper design of the error correction capabilities of the physical layer transmission. That is, for transmission standards of today, the depth of the interleaver and the error-correcting requirements of the Reed-Solomon FEC can be determined if the dynamics of the burst-error generation is known for all cases. As the frequency distribution varies, the power required of the FEC required to mitigate the beat effects also changes.

Further quantification of the phenomenon associated with the distribution of frequencies is in progress.

Optics

Most of the measurements taken so far have been done with distortion generated via RF saturation, in some cases combined into the QAM channel, and in some cases existing because of a loaded cascade. The RF signature of the beat distortion represents an important piece of the puzzle. However, the addition of the optical link enables two important impairments: clipping and second order (CSO) distortion. Second order distortion has been looked at, but has not been the main focus of the study, as this is less significant of a problem in RF-generated distortion. However, because of the importance of second order effects in optics, more focus on CSO is expected.

In terms of CTB, a shift in PDF characteristics is expected as the soft clipping

distortion mechanism of RF amplifiers is augmented with the hard clipping distortion. Both soft clipping and hard clipping are functions well studied regarding their effects on signal statistics. Furthermore, nonlinear circuits (pre-distorters) designed specifically for CTB mitigation can impact characteristics.

NCTA Definitions

A primary inspiration for these studies is to develop, crudely, a test procedure modification, at it simplest a "fudge factor" that can be used to correlate measured distortion performance via the NCTA definition to successful 256-QAM performance. Indications are that, because there are multiple impairments that 256-QAM exhibits high sensitivity to, this may be difficult except under very controlled circumstances (like can be achieved in a lab but not in the field).

Other Variables

The nature of either of the distortion beats can be characterized using the methods described here. There are compelling reasons to evaluate the same system implications of the CSO, particularly as measurements move away from RF only. Taking BER measurements with pure CSO and pure CTB would be informative.

Other obvious variables in the composite signal load include ratio of analog to digital levels, frequency, and composite load variation.

SUMMARY AND CONCLUSIONS

For systems that carry both traditional analog video channels in combination with digital QAM signals, the usual NCTA method of measuring distortions are inadequate to ensure robust error-free reception of the digital channels. The statistical properties of the distortion beats as described by the probability density function and its associated cumulative distribution function play a role in determining the acceptable level of the distortion beat falling within the digital channel.

We began with some field data to show the level of visible impairments in the pictures, and followed it with early lab evidence to separate the influence of intermodulation distortion. These early experiments gave evidence of one broad conclusion, that the sensitivity of QAM channel to CTB created by modulated carriers was higher than that of the CTB generated by CW tones. They further showed the need to characterize the bursty nature of the composite distortions.

We began the more thorough characterization with the development of a measurement technique to capture the data from distortion beats in a manner which facilitated analysis and experimental comparison. The body of the paper contains the details of these setup issues and caveats for their use, as well as recommended spectrum analyzer bandwidth and mode settings. The essence of the technique is to use the spectrum analyzer as a tuned receiver and capture the video data on a fast oscilloscope with histogram capability for further evaluation. The instantaneous amplitude of the distortion beat outputs were compared to several "typical" distribution functions, the best matched of which was the Rayleigh distribution. This was true regardless of average value measured via NCTA methods. This same output was analyzed with mathematical analysis software to determine its frequency content via FFT. The FFT data clearly show the band limitations selected by the measurement equipment and the additional CSO beat just beyond the band edge.

Quantitative results from the experimental data comparing 64 and 256-QAM are found most readily in Figure 12. To reiterate, 256-QAM is 6 dB more sensitive to AWGN compared to 64-QAM. However, under the conditions tested here it showed 14 dB more

sensitivity to CTB and CSO from live video and 11 dB more sensitivity to CTB and CSO from CW tones. This sensitivity is heightened as the interference level drops.

Analytical interpretations and the qualitative match with experimental data were considered next. It is here that the Rayleigh distribution is fit to the data, and background and significance are explained. Models of various types of interference were described, along with the assumptions and their limitations. Geometric interpretations of CW single interferers and AWGN for 64-QAM and 256-QAM were also given. These were followed by analytical BER evaluations and an approach to understand CTB in terms of the analysis, and hence BER as a function of the CTB.

Lab measurements of BER for various levels of S/I were presented, and show that that 64-QAM is approximately 12 dB more robust to a single interfering tone regardless of whether the tone was at the center frequency of a channel or at a location consistent with a CTB beat. These data, the earlier field data, the analytical indications, and the comparison of live video to CW tones show fairly consistently that for low levels of live video interferers, 256QAM will be more sensitive by this 12-14 dB. Measurements of RF amplifier cascades at various temperatures show the functional dependence of 256-QAM BER on level of interference, and the addition of a fiber optic link demonstrate the importance of considering all the sources of impairment . In particular, laser clipping limits the attainable level of BER for a given level of interference compared to that of an RF cascade alone.

In conclusion, we are beginning to make headway toward answering the question of how to define completely the relative level of a distortion beat that impairs a digital (QAM) channel. Instantaneous distributions of distortion beats are certainly a factor in answering this question, but not totally independent of the type and source of interfering signals. In addition, the methods of forward error correction will have more or less influence again depending on the various types, sources, and levels of the interference.

Looking ahead, it is clear that further work will be required in fiber optic links, especially to quantify the impairment induced by clipping. Expected variations in the PDF of distortions need to be quantified, as does the influence of the source frequency variation. Plans for further work also include the influence of various channel plans, number of analog versus digital channels, relative phasing of the frequency sources, and quantification and interpretation of time domain data including number, distribution, and duration of peaks leading up to and following a "trigger" from a particular amplitude interfering event. Finally, more complete data on the effects of CW to QAM power and the relationship to average power of a distortion beat as measured by NCTA methods will be pursued, as will the influence of cascade depth and optical links. It is anticipated that a comprehensive interpretation of influences on QAM BER will lead to greater understanding of today's components, systems, and their interaction and will help to suggest elegant solutions to overcome limitations.

ACKNOWLEDGEMENTS

We would like to acknowledge the following individuals for their valuable contributions to this paper, and their continued efforts on this program: Javier Borlando, Vipul Rathod, Mike Short, and Joe Waltrich

---

[i] NCTA Recommended Practices for Measurements on Cable Television Systems, Second edition, revised October 1993